Effect of Annealing Temperature on Back Electron Transfer and Distribution of Deep Trap Sites in Dye-Sensitized TiO_2, Studied by Time-Resolved Infrared Spectroscopy

Kan Takeshita* and Yutaka Sasaki

Center for Analytical Chemistry and Science, Inc., 1000 Kamoshida-cho, Aoba, Yokohama 227-0033, Japan

Masahiro Kobashi, Yuki Tanaka, and Shuichi Maeda

Science and Technology Research Center, Mitsubishi Chemical Corporation, 1000 Kamoshida-cho, Aoba, Yokohama 227-8502, Japan

Akira Yamakata, Taka-aki Ishibashi, and Hiroshi Onishi

Surface Chemistry Laboratory, Kanagawa Academy of Science and Technology (KAST), KSP East 404, 3-2-1 Sakado, Takatsu, Kawasaki 213-0012, Japan

Received: May 22, 2003; In Final Form: December 26, 2003

The effect of annealing temperature on electron dynamics in Ru complex-sensitized TiO_2 films was studied by highly sensitive measurement of transient IR absorption. The amount of electron injection and the back electron transfer rate were not influenced to a large extent by annealing temperature, but the distribution of deep trap sites was considerably influenced. The difference in solar cell efficiency due to annealing temperature was mainly attributed to the difference in the nature of deep trap sites. By extending the probe light window from the mid-IR (1000−4000 cm^{-1}) to the near-IR (−10000 cm^{-1}) region, we investigated deep trap sites directly and found that electrons in deep trap sites have absorption in the near-IR region whose peak locates around 7500 cm^{-1}. As a whole, the electron dynamics in the films annealed at higher than 400 °C were considerably different compared with those in the films annealed at lower than 400 °C.

1. Introduction

Over the past few decades, a considerable number of studies have been conducted on interfacial electron transfer between molecular adsorbate and semiconductor substrates.[1−5] These studies have been done because of the promising application for photovoltaic cells[6] as well as for scientific interest. For efficient solar energy conversion, it is important to understand the forward and backward electron transfer processes, especially their dynamics in semiconductor nanoparticles and molecular adsorbates. To achieve high efficiency for converting absorbed light into electricity, we need fast electron injection from the adsorbate to the semiconductor and fast collection of injected electrons into electrodes compared with the back electron transfer. Recently, femtosecond spectroscopy has been used to study the interfacial electron transfer processes by directly monitoring the injected electrons in the semiconductor and also by observing the bleach of the adsorbate.[7−13] These studies have revealed that the electron injection rate from the excited state of adsorbate to the semiconductor conduction band is much faster than the deactivation rate of the excited state of the adsorbate. These observations mean that the initial electron injection from the adsorbate to the semiconductor is very efficient.

Since initial electron injection has been proved to be quite efficient and not so dependent on materials, much more attention has been paid to the postinjection process and the factors that determine these rates. The postinjection process has also been studied extensively,[14−19] but many of these studies have focused only on back electron transfer. This is because these studies were done by measuring bleach recovery of the adsorbate with transient absorption in the visible light range, and electrons in the semiconductor cannot usually be detected by visible light. Apart from back electron transfer, however, there are other important electron processes in semiconductors, such as diffusion or relaxation to trap sites.

In our previous work,[20] we demonstrated the ability of transient mid-IR absorption spectroscopy in tracing μs kinetics of the postinjection processes. Electrons photoexcited and trapped at shallow mid-gap states presented a structureless absorption when thermally excited from the traps to the conduction band.[21] The ionized fraction of the dye molecule was, on the other hand, observable by the intensity of a vibrational band assigned to the cationized dye. The decay rate of the shallow-trapped electron and the neutralization (i.e., back electron transfer) rate of the dye cation were thereby independently determined; the former was larger than the latter. To interpret this observation, the decay of the shallow-trapped electrons into deep traps undetectable by the mid-IR absorption was proposed. It is important to characterize these trap states, because they control the postinjection processes and thus the solar cell efficiency.[22−28]

In the present work, we observed the electron kinetics of dye-sensitized films annealed at different temperatures. Annealing prior to dye-sensitization is assumed to heal trap states that should be localized on particle boundaries, lattice dislocations, the amorphous portion in each particle, and atom vacancies.[27−29] Another experimental improvement in the present work is the

* To whom correspondence should be addressed. E-mail: 5503103@cc.m-kagaku.co.jp. Phone: +81-45-963-3155. Fax: +81-45-963-4261.

10.1021/jp035416o CCC: $27.50
Published on Web 02/07/2004

extended probe light window from the mid-IR (1000−4000 cm^{-1}) to the near-IR (−10000 cm^{-1}) region. If optically allowed, the direct transition from the deep traps to the conduction band can be observed by absorption of the near-IR light.

2. Experimental Section

Sample Preparation. TiO_2 nanocrystalline thin films were prepared by a method similar to that used by Nazeeruddin and co-workers.[30] Briefly, a TiO_2 colloid solution was made from TiO_2 powder (P25 Degussa), water, and small amounts of acetylacetone and detergent (Triton X-100). The colloid solution was spread on a CaF_2 plate substrate using a glass rod. After air-drying, the plate was sintered for 30 min at 200−600 °C in air. The sensitizing dye used in this study was ruthenium complex N3; $Ru(dcbpy)_2(NCS)_2$ [dcbpy = (4, 4′-dicarboxy-2,2′-bipyridine)]. This Ru complex was dissolved in a mixture solvent (1:1) of butanol and acetonitrile. The TiO_2 films were immersed in the dye solution at room temperature to fix the dye onto the surface. The immersion time was controlled in order that the absorbance of samples was around 1.0 at the excitation wavelength.

Transient IR Absorption Measurement. We used systems and procedures similar to those reported by Iwata et al.[31] and Yamakata et al.[21] for transient IR absorption spectrum measurements. Briefly, the light emitted from a halogen lamp or a $MoSi_2$ infrared source was focused on the sample plate with ellipsoidal mirrors. The halogen lamp and the $MoSi_2$ infrared source were used for 10000−4000 and 4000−1000 cm^{-1} measurements, respectively. The transmitted light was dispersed in a monochromator (JASCO, CT50TF) of 50 cm focal length. Gratings of 300 or 100 grooves/mm were used for 10000−2000 and 2000−1000 cm^{-1} measurements, respectively. The monochromatic output was detected by a low-noise photovoltaic MCT detector (Kolmar). The signal output was amplified in AC-coupled amplifiers and accumulated in a digital sampling oscilloscope (Lecroy, LT342L) as a function of delay time at a fixed wavelength. The temporal profiles were reconstructed to time-resolved absorption spectra at different delay times. The time-resolution of the instruments was about 50 ns. The excitation pulse was the second harmonic of a Q-switched Nd:YAG laser (532 nm). The excitation pulse energy was 0.2−1 mJ/cm^2. Transient absorbance change as low as 10^{-6} was detected by signal averaging about 100−300 times at 5 Hz.

3. Results

3.1. Comparison of the Transient Absorption Spectra in the Mid-IR Region among TiO_2 Films Annealed at Different Temperatures. The transient absorption of N3-sensitized TiO_2 film in the mid-IR region was reported previously by Asbury et al.[10] (fs−ps pump−probe detection) and by our group[20] (CW probe detection). Figure 1 shows our result of a transient absorption of N3-sensitized TiO_2 film annealed at 400 °C. After a pulse excitation, a broad unstructured absorption appeared over the range measured. This broad absorption is attributed to electrons injected from the LUMO of N3 to the conduction band of TiO_2. Besides the broad background absorption, a change in the CN stretching mode of N3 was observed around 2100−2000 cm^{-1}. The excitation led to bleaching of the ground-state absorption at 2110 cm^{-1} and creation of two new bands at 2025 and 2070 cm^{-1}. We reported in the previous paper the discrepancy between the decay of the broad background absorption and the 2025 cm^{-1} peak. Since the 2025 cm^{-1} peak originates from the N3 cation C−N stretch band, it disappears only when the injected electrons revert to N3. Therefore, the decay of the 2025 cm^{-1} peak reflects the back electron transfer rate. On the other hand, the broad background absorption represents the electrons in the conduction band or shallow traps (which are thermally equilibrated to the conduction band) of TiO_2. It disappears through two paths; one is back electron transfer and the other is decay to other sites in the semiconductor not detected by mid-IR light. Consequently, the background absorption decays faster than the N3 cation C−N stretch band.

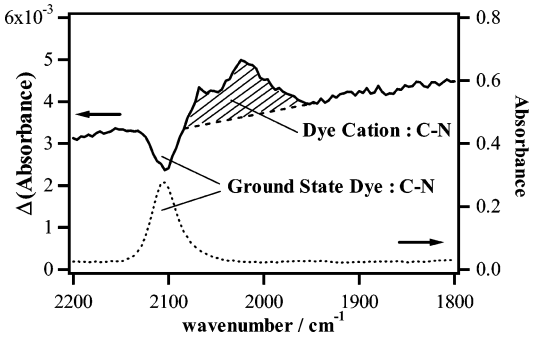

Figure 1. Steady-state absorption spectrum (dotted line) and transient absorption spectrum (solid line) of N3-sensitized TiO_2 around 2000 cm^{-1}. (Adapted from the previous report.[20])

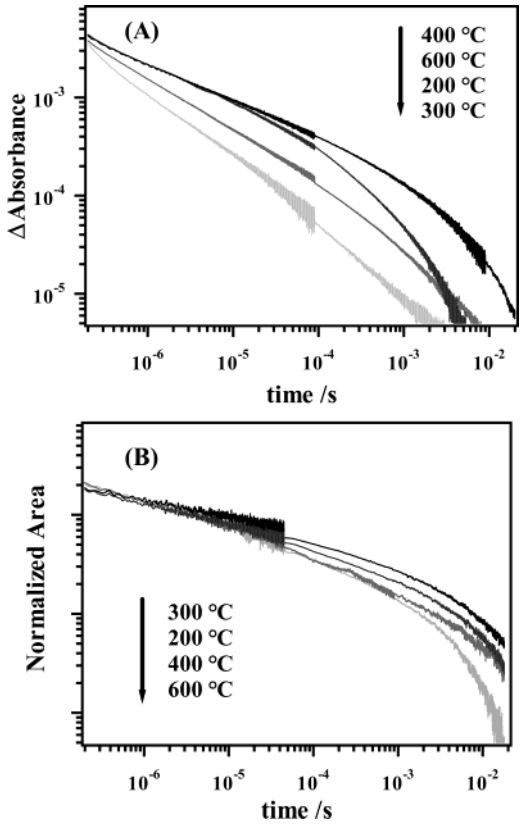

Figure 2. Dependence of the decay of the transient absorption at 1950 cm^{-1} (A) and N3 cation C−N stretch band (B) on the annealing temperature.

Figure 2 shows temporal profiles of the background absorption and C−N stretch band of N3-sensitized TiO_2 annealed at different temperatures. As mentioned above, the background absorption (differential absorbance value at 1950 cm^{-1} represents the intensity of the background absorption) decayed faster than the area of the N3 cation C−N stretch band at any annealing temperatures. In addition, there was a large difference in the dependence on the annealing temperature for these two signals. The decay profile of the background absorption depended on the annealing temperature, whereas that of the N3

TABLE 1: Initial Intensity of the Transient Absorption at 1950 cm^{-1} (relative value[a])

annealing temperature	intensity
200 °C	0.86
300 °C	0.84
400 °C	1
600 °C	0.96

[a] The values are normalized as the value of the 400 °C sample becomes unity. The difference in the amount of absorbed photons among difference samples is calibrated by the sample absorbance value.

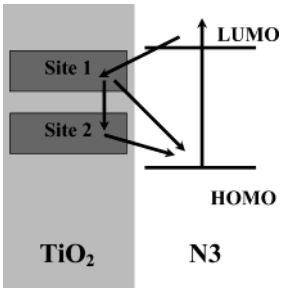

Figure 3. Model for electron processes in the N3-sensitized TiO_2 after injection to explain our mid-IR transient absorption measurement.

cation C−N stretch band did not show this dependence to the same extent. The latter observation means the back electron-transfer rate from TiO_2 to N3 was not influenced by annealing temperature, because the decay of the N3 cation C−N stretch band directly reflects the back electron transfer. On the other hand, the decay of the background absorption represents more complicated processes including trapping, which were probably influenced by the annealing temperature. Since electron trapping in the semiconductor has a relation to the number and the distribution of the trap sites, it must be affected by annealing temperature. It was rather surprising that only a 100 °C gap in annealing temperature made such a large difference in the decay of the background absorption. (See the signals for 300 °C and 400 °C in the Figure 2B.) At first, we suspected that other factors besides annealing temperature (such as thickness or absorbance of a sample) might also affect the signal. However, the results shown in Figure 2B were reproduced well only by the difference in the annealing temperature.

The signals shown in Figure 2 provide one more important piece of information. The initial intensity of background absorption (Figure 2A) should be proportional to the amount of electron injection. We can evaluate the relative amount of electron injection in different samples by comparison of the initial intensity of signals shown in Figure 2A. This comparison is shown in Table 1, which indicates there was no notable difference in the amount of electron injection by annealing temperature.

To consider in more detail postinjection processes from the data shown in Figure 2, we introduce a simple model for electron processes in the dye-sensitized semiconductor after injection (Figure 3). Because we have already explained the same model in a previous paper,[20] only essential points are briefly reviewed here. In this model, we separate the sites in the semiconductor into the following two types:

(i) Site 1: Electrons in this site give uniform absorption for mid-IR light (conduction band and shallow traps correspond to this site).

(ii) Site 2: Electrons in this site give no absorption for mid-IR light (deep traps and surface states correspond to this site).

We assume that all electrons are initially injected into site 1 from the LUMO of the sensitized dye and that these electrons revert to the HOMO of the sensitized dye directly or via site 2. On that assumption, we can use the following method to estimate the population of electrons in sites1 and 2 as a function of time. The background absorption in Figure 2a reflects the number of electrons in site 1 (the decay curves themselves are relative electron quantity in site 1), whereas the area of the dye cation C−N stretch band in Figure 2b reflects the number of electrons both in sites 1 and 2. Consequently, if we normalize these two signals at time zero and subtract the former from the latter, we can obtain the relative electron population in site 2 as a function of time.

Figure 4 depicts the relative electron population in sites 1 and 2 as a function of time in the samples annealed at different temperatures (they are normalized, as the population of site 1 becomes 1 at time zero). In all samples, the population of site 1 shows nonexponential decay and the population of site 2 shows a growth-decay profile. There is a distinct difference in the temporal profiles of population in site 2 according to annealing temperature. When TiO_2 was annealed at 200 and 300 °C, more electrons passed through site 2 than when annealed at higher temperature. This phenomenon probably stems from the fact that more trap sites are formed at a low annealing temperature than at a high one. The detailed relationship between annealing temperature and trap sites is discussed in the section 4.

3.2. Extension of Transient Absorption Spectra to the Near-IR Region. In the previous section, we mentioned the deep trap sites in TiO_2. However, these trap sites were not directly observed. We only presumed the existence of deep trap sites from the discrepancy of decay between the background absorption in the mid-IR region and the C−N stretch band of the adsorbate cation. If the deep trap sites are not detected by mid-IR in terms of energy (their energy levels are too low from the edge of the conduction band to absorb mid-IR light), they may be detected by high wavenumber (energy) light. Hence, we report the extension of our transient absorption spectra to the near-IR region in this section.

Figure 5A shows the transient absorption spectrum of N3-sensitized TiO_2 (annealed at 400 °C) in the region of 1000−10000 cm^{-1}. (The time evolution of this spectrum is also shown.) In the near-IR region (>4000 cm^{-1}), a broad absorption band was observed around 7500 cm^{-1}. We also found the decay of this peak was fairly different from the mid-IR transient absorption. This decay difference is shown in Figure 5B with the decay of the N3 cation C−N stretch band. (In Figure 5b, 1950 cm^{-1} represents the mid-IR region and 7500 cm^{-1} represents the near-IR region.) The decay of the transient absorption at the near-IR region was considerably slower than that at the mid-IR region. Instead, it resembles the decay of the N3 cation C−N stretch band. In semiconductors, electrons in deep trap sites give absorption bands by a direct transition from trap sites to a conduction band.[32] Therefore, we tentatively ascribed the 7500 cm^{-1} band to the absorption of electrons in deep traps sites in TiO_2.

In N3-sensitized TiO_2, however, some groups have observed the injected electron absorption on the fast time scale (fs−ps) in the near-IR region.[33] The observed electrons in ref 33 should not be decayed into deep traps on this time scale. Instead, this absorption should be ascribed to electrons in the conduction band and the shallow trap sites. This fact implies that our transient absorption in the near-IR region contains also the "conduction band and shallow traps" component. Consequently, we concluded that our transient near-IR absorption represents

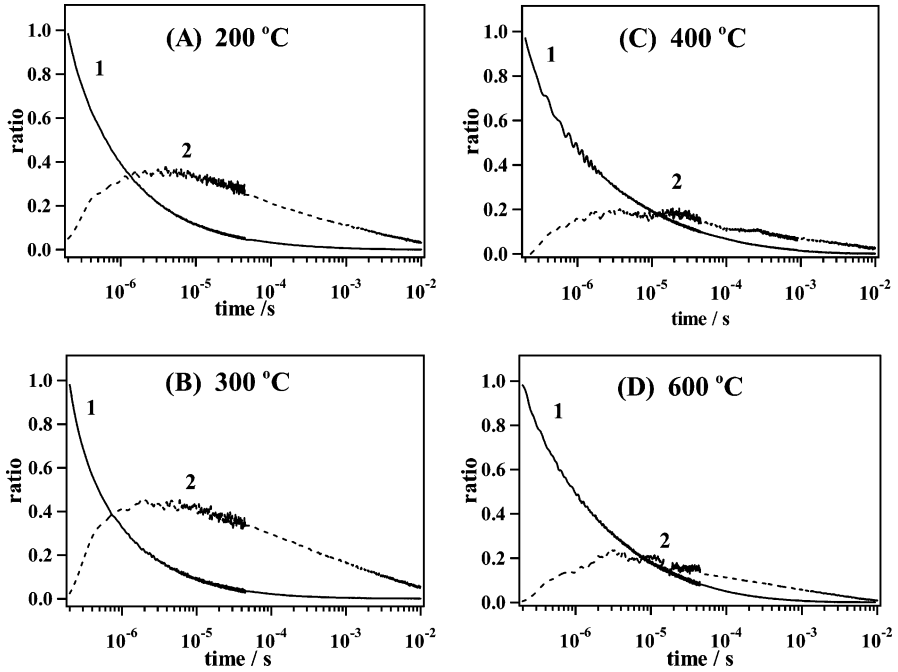

Figure 4. Transition of population in sites 1 and 2 in Figure 3 calculated from the difference in the decay between the background absorption and the C−N stretch band. Each chart depicts the population profile for the sample annealing at 200 (A), 300 (B), 400 (C), and 600 °C (D).

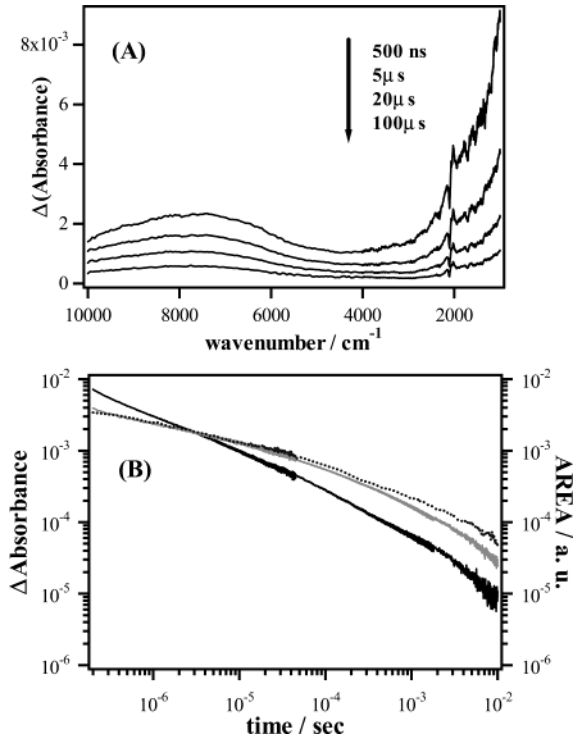

Figure 5. (A) Transient absorption spectrum of N3-sensitized TiO_2 after a pulse excitation at 532 nm from mid-IR to near-IR. (B) Decay profiles of the transient absorption at 1950 (black solid line) and 7500 cm^{-1} (gray solid line) and the area of the C−N peak of a dye cation (black dotted line).

the absorption of both "conduction band and shallow trap sites" and "deep trap sites".

Here we try to separate the deep trap sites component from the total transient absorption. In the case of platinized TiO_2 or naked TiO_2, excitation by UV pulse gives rise to the transient absorption represented by the following equation:[21]

$$\Delta\text{absorbance} = A\tilde{\nu}^{-1.5} \qquad (1)$$

where A is a constant and $\tilde{\nu}$ is the wavenumber of IR light. This transient absorption is assigned to electrons in the conduction band and shallow mid-gap states. We found that the mid-IR region (<4000 cm^{-1}) of the transient absorption of N3-sensitized TiO_2 was almost identical with platinized TiO_2 except the vibration band changes of N3 dyes. Therefore, we assume that the "conduction band and shallow traps" component is expressed by eq 1 also for the transient absorption of N3-sensitized TiO_2. Since we measured the time evolution of the transient absorption spectrum of N3-sensitized TiO_2, we can calculate the deep trap sites component and its temporal profile by subtracting the "conduction band and shallow traps" component from the total transient absorption. The calculation results are shown in Figure 6. Figure 6A is the "conduction band and shallow traps" component calculated with eq 1. Figure 6B is the residue of the observed transient absorption spectrum after subtracting the component shown in Figure 6A. Hence, Figure 6B represents the deep traps component. We also reconstructed the decay of these two components from the temporal profile of the spectra (Figure 6C). The decay difference between these two components supports our model proposed in the previous section (Figure 3). In that model, the electrons injected into site 1 decay to the HOMO of the sensitized dye directly or via site 2, which means that the electrons in site1 decay faster than the electrons in site 2.

In Figure 7, we show the result of transient absorption measurement expanded to the near-IR region for the samples annealed at different temperatures. Figure 7A shows the overall transient absorption spectra in 1000−10000 cm^{-1}. The transient absorption spectra have almost the same shape in the mid-IR region regardless of annealing temperature, whereas they give considerably different peaks in the near-IR region. The intensity and the position of the peak in the near-IR region depended on annealing temperature. However, we cannot establish any particular rules about this difference.

Figure 7B shows the comparison of the signal decay at 7500 cm^{-1}. According to Figure 6, the relative contribution of the shallow trap states to absorbance is low at 7500 cm^{-1} compared with contribution of the deep trap states. Therefore, the lines in

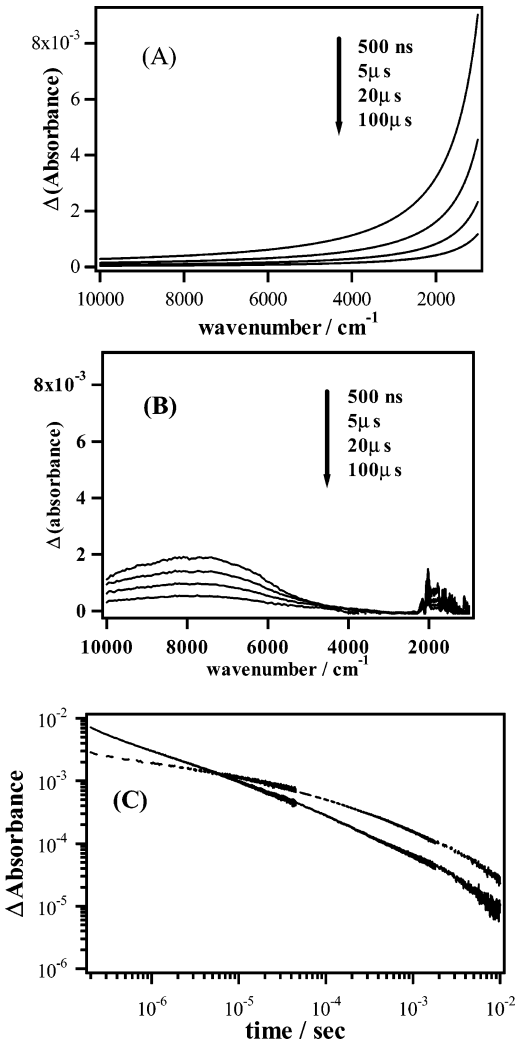

Figure 6. (A) Transient absorption of electrons in the conduction band and the shallow trap sites estimated from eq 1. (B) Estimated transient absorption of electrons in the deep trap sites. (C) Decay difference between "the conduction band and the shallow trap sites" (solid line) and the deep trap sites (broken line).

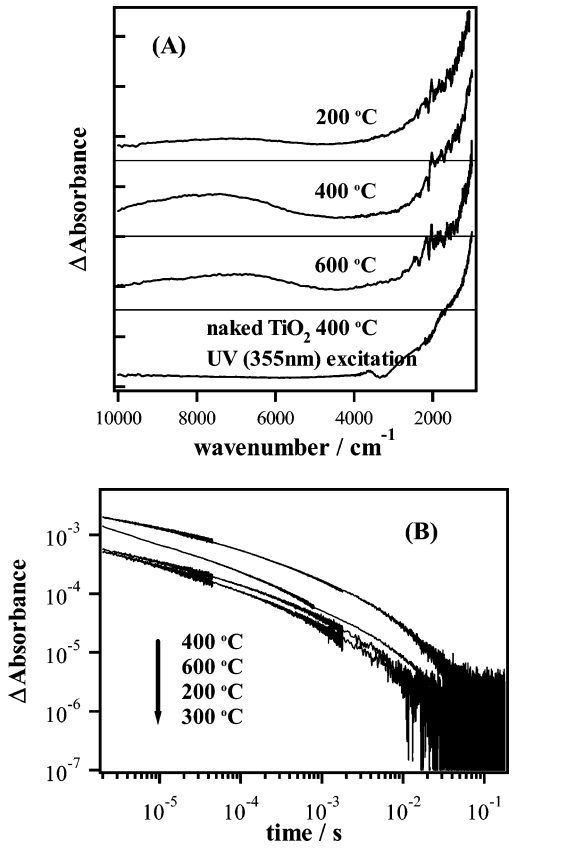

Figure 7. (A) Transient absorption spectra of N3-sensitized TiO_2 films annealed at various temperatures at 5 μs after the pulse excitation. Transient absorption spectrum of naked TiO_2 is also shown. (B) Dependence of the decay of the transient absorption at 7500 cm^{-1} on the annealing temperature.

Figure 7B approximately reflect the amount of electrons in deep trap sites. The initial amplitudes just after the instrument response time observed at 400 and 600 °C were large compared to those at 200 and 300 °C. These data suggest that electrons can relax to the deep trap states within the instrument response time, probably more for the films sintered at 400 and 600 °C. This result seems to be contradictory to the results shown in Figure 4, where we have discovered that more deep traps that could not be detected by mid-IR light were formed at 200 and 300 °C. However, the results in Figures 4 and 7B can be consistently interpreted as shown below.

In Figure 4, we assume that there is no electron population just after photoexcitation (= instrument response time). On the other hand, Figure 7B shows that electrons have already decayed to deep trap states to a certain extent within instrument response time. Therefore, the analysis shown in Figure 4 does not necessarily give the precise population of electrons in deep trap states. Instead, Figure 4 depicts only the transient electron occupation to the deep trap sites. From comparison between Figures 4 and 7B, we can conclude the following thing about electrons in deep trap states: Within instrument response time, the number of electrons in deep trap states is larger in the films annealed at 400 and 600 °C than in the films annealed at 200 and 300 °C. On the contrary, the number of electrons that decay from shallow trap states to deep traps site *after* instrument response time is larger for the films annealed at 200 and 300 °C. However, we have to pay attention the following proposition: Can all deep trap states be monitored by near-IR light? We cannot eliminate the possibility that electron in deep trap states are partially detected by near-IR light and that some electrons are not detected even by near-IR light. The discussion above is valid only if all deep trap states can be monitored by near-IR light.

The results in Figures 4 and 7B can be also explained by assuming the existence of deep trap sites that are not detected even by near-IR light. That is, we assume that there are at least two distinct types of deep trap states. One is a deep trap in which an electron is detected not by mid-IR but by near-IR; the other is deep trap in which an electron is detected neither by mid-IR nor by near-IR light. Under this assumption, we can say that only *partial* electrons in deep trap states were monitored in Figure 7B, whereas line 2 in Figure 4 shows *all* electrons in deep trap states. This is another possible interpretation of Figures 4 and 7B. However, finding out which interpretation correctly describes electron dynamics will be left to a further study.

4. Discussion

There is controversy over whether the trap sites positively or negatively affect solar cell performance.[22−28] The electron dynamics in a dye-sensitized solar cell are sometimes explained by trapping models.[28] In this model, the increase of trap sites slows the back electron transfer rate because electrons have less chance to encounter holes (dye cations) under the existence of

many trap sites. Therefore, in this model, trap sites positively affect solar cell performance. On the other hand, several studies have reported that trap sites negatively affect solar cell performance.[29,34] In these papers, this phenomenon is explained by the decrease of the diffusion constant of electrons. It is also explained by the dominance of back electron transfer via trap sites rather than direct recombination from the conduction band. Our transient absorption data might give one clue to solve this question, because we observed that the distribution of deep trap sites was considerably influenced by annealing temperature and found that it was closely correlated with the difference in solar cell performance.

The results shown in Figures 4 and 7B indicate that the border temperature that determines the behavior of the electron in deep trap sites (site 2 in Figure 3) exists between 300 and 400 °C. This fact is notable because it is strongly related to the solar cell performance. The effect of annealing temperature on solar cell performance has been studied by several groups.[29,34,35] The performance of low-temperature annealed films has shown lower efficiency than that of high-temperature annealed films. TiO_2 films for dye-sensitized solar cells are typically annealed at 400−500 °C.[29,30] If TiO_2 films are annealed below this temperature, the photon-to-current efficiency decreases. Therefore, 400−500 °C is the minimum annealing temperature for sufficient utilization of the ability of dye-sensitized TiO_2 films. The decrease of efficiency at a low annealing temperature has been partially explained by the change in diffusion coefficients of electrons in nanoporous films.[29,34,35] Nakade et al. reported that the diffusion coefficients increased with annealing temperature and that this was due to the charge-trap density and neck growth between particles.[29] From these points of view, our analysis shown in Figure 4 is interesting. Our results indicate that the number of electrons that decay to deep trap sites after instrument response time increases when TiO_2 films are annealed below 400 °C, the typical annealing temperature. We again emphasize that the back electron transfer rate did not depend on the annealing temperature in our experiment. The only difference caused by the annealing temperature was the number and the temporal profile of electrons that pass through deep trap sites. Consequently, the decrease of solar cell performance at an annealing temperature lower than 400 °C must have a strong relation to these deep trap sites.

Electron traps are derived from native defects due to oxygen deficiency and adsorbed species on a large film surface area.[28] These states result from the localization of an electron in the Ti 3d orbital in the presence of an electron donation defect.[36,37] The location of the trap states in semiconductor electrodes may be either in the bulk, at grain boundaries, or at the semiconductor/adsorbate interface (surface states). In our experiment, we observed electrons in both shallow and deep trap sites in N3-sensitized TiO_2. It is rather difficult to identify the location of each trap state. However, we have one clue about deep trap states. We measured the transient absorption spectrum for naked TiO_2 in the near-IR region as shown in Figure 7. The peak observed in N3-sensitized TiO_2 was not recognized. Therefore, this peak is formed only if the sensitizing dye is attached. Katoh et al. measured the near-IR transient absorption spectrum for N3-sensitized ZnO.[38] In the case of N3-sensitized ZnO, the spectrum did not have the peak observed in N3-sensitized TiO_2. Accordingly, this deep trap may be formed by the Ti orbital and the O orbital of N3. These trap sites affect interfacial kinetics and strongly correlate with solar cell performance. However, it is known that the distribution of trap sites is influenced by an electrolyte solution.[25,27,28] Therefore, to study more precisely the relationship between trap sites and solar cell performance obtained in this work, we will need an additional experiment in the presence of an electrolyte solution.

5. Summary

The electron processes after injection in Ru complex-sensitized TiO_2 were investigated by the transient IR absorption method. We particularly aimed at examining the effect of annealing temperature on electron dynamics. We found that the number of injected electrons and the back electron transfer rate were not influenced by annealing temperature but that the distribution of deep trap sites was considerably influenced. By extending the probe light window from the mid-IR to the near-IR region, we found that some of the electrons in deep trap sites have absorption in the near-IR region whose peak locates around 7500 cm^{-1}. These deep trap sites were probably formed by interaction between the TiO_2 surface and the adsorbate. Electron dynamics in the films annealed at higher than 400 °C were considerably different compared with those in the films annealed at lower than 400 °C. This fact is particularly interesting because it is strongly related to solar cell performance.

Acknowledgment. This work was supported by Core Research for Evolutional Science and Technology of Japan Science and Technology Agency. We are also grateful for financial support by CREST of the Japan Science and Technology Corporation and a Grant-in-Aid for Scientific Research from the Ministry of Education, Culture, Sports, Science and Technology of Japan (No. 15655077).

References and Notes

(1) Gerischer, H.; Michel-Beyerle, M. E.; Rebentrost, F.; Tributsch, H. *Electrochim. Acta* **1968**, *13*, 1509.
(2) Gerischer, H. *Photochem. Photobiol*. **1972**, *16*, 243.
(3) Hagfeldt, A.; Grätzel, M. *Chem. Rev*. **1995**, *95*, 49.
(4) Nozik, A. J.; Memming, R. J. *J. Phys. Chem*. **1996**, *100*, 13061.
(5) Kamat, P. V.; Meisel, D. *Semiconductor Nanoclusters-Physical, Chemical, and Catalytic Aspects*; Elsevier: Amsterdam, 1997; Vol. 103.
(6) O′Regan, B.; Grätzel, M. *Nature* **1991**, *353*, 737.
(7) Tachibana, Y.; Moser, J. E.; Grätzel, M.; Klug, D. R.; Durrant, J. R. *J. Phys. Chem.* **1996**, *100*, 20056.
(8) Martini, I.; Hodak, J.; Hartland, V. *J. Chem. Phys.* **1997**, *107*, 8064.
(9) Ellingson, R. J.; Asbury, J. B.; Ferrere, S.; Ghosh, H. N.; Sprague, J. R.; Lian, T.; Nozik, A. J. *J. Phys. Chem. B* **1998**, *102*, 6455.
(10) Asbury, J. B.; Ellingson, R. J.; Ghosh, H. N.; Ferrere, S.; Nozik, A. J.; Lian, R. *J. Phys. Chem. B* **1999**, *103*, 3110.
(11) Asbury, J. B.; Hao, E.; Wang, Y.; Ghosh, H. N.; Lian, R. *J. Phys. Chem. B* **2001**, *105*, 4545.
(12) Heimer, T. A.; Heilweil, E. J.; *J. Phys. Chem. B* **1997**, *101*, 10990.
(13) Heimer, T. A.; Heilweil, E. J. *Proceedings for Ultrafast Phenomena XI*; Springer-Verlag: Berlin, 1998; pp 505−507.
(14) O'Regan, B.; Moser, J.; Anderson, M.; Grätzel, M. *J. Phys. Chem.* **1990**, *94*, 8720.
(15) Haque, S. A.; Tachibana, Y.; Willis, R. L.; Moser, J. E.; Grätzel, M.; Klug, D. R.; Durrant, J. R. *J. Phys. Chem. B* **2000**, *104*, 538.
(16) Heimer, T. A.; Heilweil, E. J.; Bignozzi, C. A.; Meyer, G. J. *J. Phys. Chem. A* **2000**, *104*, 4256.
(17) Haque, S. A.; Tachibana, Y.; Klug, D. R.; Durrant, J. R.*J. Phys. Chem. B* **1998**, *102*, 1745.
(18) Kuciauskas, D.; Freund, M. S.; Gray, H. B.; Winkler, J. R.; Lewis, N. S. *J. Phys. Chem. B* **2001**, *105*, 392.
(19) Willis, R. L.; Olson, C.; O'Regan, B.; Lutz, T.; Nelson, J.; Durrant, J. R. *J. Phys. Chem. B* **2002**, *106*, 7605.
(20) Takeshita, K.; Sasaki, Y.; Kobashi, M.; Tanaka, Y.; Maeda, S.; Yamakata, A.; Ishibashi, T.; Onishi, H. *J. Phys. Chem. B* **2003**, *107*, 4156.
(21) Yamakata, A.; Ishibashi, T.; Onishi, H. *Chem. Phys. Lett.* **2001**, *333*, 271.
(22) Schwarzburg, K.; Willig, F. *Appl. Phys. Lett.* **1991**, *58*, 2520.
(23) Boschloo, G. K.; Goossens, A. *J. Phys. Chem.* **1996**, *100*, 19489.
(24) de Jongh, P. E.; Vanmaekelbergh, D. *Phys. Rev. Lett.* **1996**, *77*, 3427.

(25) Franco, G.; Gehring, J.; Peter, L. M.; Ponomarev, E. A.; Uhlendorf, I. *J. Phys. Chem. B* **1999**, 103, 692.
(26) van de Lagemaat, J.; Frank, A. J. *J. Phys. Chem. B* **2001**, 105, 11194.
(27) Wang, H.; He, J.; Boschloo, G.; Lindström, H.; Hagfeldt, A.; Lindquist, S.-E. *J. Phys. Chem.* **2001**, *105*, 2529.
(28) Nelson, J.; Haque, S. A.; Klug, D. R.; Durrant, J. R., *Phys. Rev. B* **2001**, *63*, 205321.
(29) Nakade, S.; Matsuda, M.; Kambe, S.; Saito, Y.; Kitamura, T.; Sakata, T.; Wada, Y.; Mori, H.; Yanagida, S. *J. Phys. Chem. B* **2002**, *106*, 10004.
(30) Nazeeruddin, M. K.; Kay, A.; Rodicio, I.; Humphry-Baker, R.; Müller, E.; Liska, P.; Vlachopoulos, N.; Grätzel, M. *J. Am. Chem. Soc.* **1993**, *115*, 6382.
(31) Iwata, K.; Hamaguchi. H. *Appl. Spectrosc.* **1990**, *44*, 1431.
(32) Pankove, J. I. *Optical Processes in Semiconductors*; Dover: New York, 1975.
(33) Benkö, G.; Kallioinen, J.; Korppi-Tommola, J. E. I.; Yartsev, A. P.; Sundström, V. *J. Am. Chem. Soc.* **2002**, *124*, 489.
(34) Park, N.-G.; Schlichthörl, G.; van de Lagemaat, J.; Cheong, H. M.; Mascarenhas, A.; Frank, A. J. *J. Phys. Chem. B* **1999**, *103*, 3308.
(35) Pichot, F.; Pitts, J. R.; Gregg, B. A. *Langmuir* **2000**, *16*, 5626.
(36) Howe, R. F.; Grätzel, M. *J. Phys. Chem.* **1985**, *89*, 4495.
(37) Cao, F.; Oskam, G.; Searson, P. C.; Siripala, J. M.; Heimer, T. A.; Farzad, F.; Meyer, G. J. *J. Phys. Chem.* **1995**, *99*, 11974.
(38) Katoh, R.; Furube, A.; Hara, K.; Murata, S.; Sugihara, H.; Arakawa, H.; Tachiya, M. *J. Phys. Chem. B* **2002**, *106*, 12957.